

Shaking table tests for seismic stability of stacked concrete blocks used for radiation shielding

Luca Sironi^a, Marco Andreini^a, Cristiana Colloca^a, Michael Poehler^a, Davide Bolognini^b, Filippo Dacarro^b, Pierino Lestuzzi^{c,*}, Frédéric Dubois^d, Ziran Zhou^e, José E. Andrade^e

^a CERN, European Organization for Nuclear Research, Esplanade des Particules 1 - 1217 Meyrin, Switzerland

^b EUCENTRE, European Centre for Training and Research in Earthquake Engineering, Via Adolfo Ferrata, 1 - 27100 Pavia, Italy

^c EPFL ENAC IIC EESD, Swiss Federal Institute of Technology Lausanne, GC B2 485 (Bâtiment GC) - Station 18 - CH-1015 Lausanne, Switzerland

^d LMGC, Université de Montpellier, CNRS, Montpellier, 163 rue Auguste Broussonnet, 34090 Montpellier, France

^e Caltech, California Institute of Technology, 1200 E. California Blvd., MC 104-44 Pasadena, CA 91125, USA

ARTICLE INFO

Keywords:

Shaking table tests
Seismic stability
Rocking
Radiation shielding
Concrete blocks
LMGC90

ABSTRACT

This paper describes the shaking table tests carried out at the European Centre for Training and Research in Earthquake Engineering (EUCENTRE) to investigate the seismic behaviour of four configurations of stacked concrete blocks, commonly used at the European Organisation for Nuclear Research (CERN) as a shielding barrier against different types of radiation. The blocks used for these configurations have been designed to guarantee an adequate level of protection to radiation and, at the same time, to be easily transported and managed for different installations. The block configuration specimens have been tested using the acceleration time-histories of two different earthquakes occurred in the Mediterranean region. Each configuration has been tested several times with acceleration amplitude increments until rigid kinematics are triggered. This paper presents the test setup and inputs, the related experimental readings and the main results obtained by these tests. The two main mechanisms observed at the interfaces between the blocks during the tests were sliding and rocking. The data collected at the end of the experimental campaign constitute an important source to calibrate different discrete-system-models, in order to study the seismic response of block configurations used for radiation protection in particle physics research institutions.

1. Introduction

Particle physics research laboratories often have the need to shield personnel, equipment and high-technology devices from radiations produced during daily functioning, such as operations of particle accelerators. The most common approach to achieve the required level of shielding is to use blocks of significant mass. Different configurations of stacked concrete blocks are commonly used for this purpose at the European Organization for Nuclear Research, abbreviated CERN.

In this context, there is the need to guarantee an adequate level of structural safety of stacked concrete block assemblies under static and dynamic loads (i.e. seismic actions). Among similar research centres around the world, CERN is one of the few that uses such blocks without any joint-connections or any additional metallic bracing systems that resist to lateral forces that might be induced during seismic excitations (Fig. 1).

This kind of particular configurations is not codified in Europe [1,2] and there is no standardized procedure to carry out a structural

safety assessment of it. From 2012 to 2019, CERN investigated the behaviour of the stacked concrete blocks subjected to seismic actions by means of theoretical methods based on analytical and numerical models for simple block piles as well as more complex configurations. Several analytical models for the prediction of the dynamic response of individual rigid blocks or simple piles during earthquake exist in literature [3–13]. Most of them were developed for applications in the refurbishment of ancient buildings and in the architectural heritage context. The models that have been adopted were oriented to predict the seismic behaviour of monolithic stone elements, recurrently present in the Greek and Roman monumental buildings [14], and equipment of significant mass [15,16]. Piles of several blocks have been treated as a single equivalent rigid block. Such a simplification has been verified on the basis of results from the analysis of ancient temple columns [14].

For what concerns multiple and complex block configurations, little has been done in terms of experimental testing. Some numerical discrete element models have been developed in the last decades [17–19].

* Corresponding author.

E-mail address: pierino.lestuzzi@epfl.ch (P. Lestuzzi).

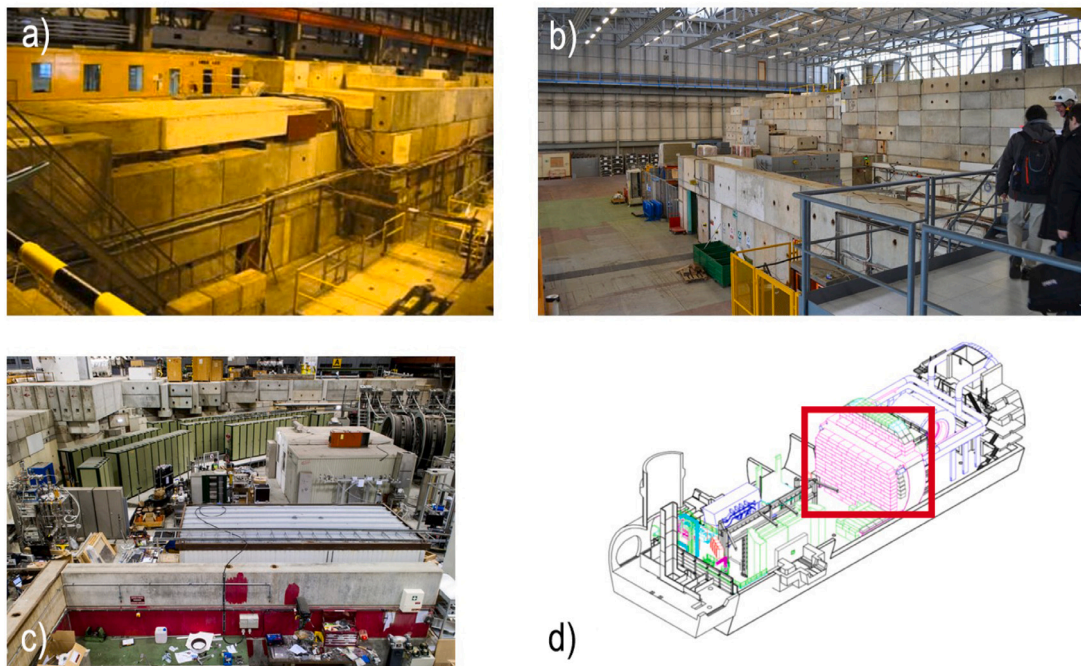


Fig. 1. Examples of concrete block configurations at CERN: (a) Experimental Hall North, (b) Eastern Area, (c) Antimatter Factory and (d) Large Hadron Collider beauty (LHCb) experiment.

Nevertheless, such models were not fully validated by experimental tests and, therefore, the bias associated to the obtained results on the analysed block configurations was not known and should be assessed.

To this end, an experimental campaign concerning shaking table tests on four different block configurations has been carried out at EUCENTRE (Pavia, Italy). This paper presents the test setup, the adopted acceleration time-histories, the measurement systems and the related experimental readings, which have been taken with the intent to calibrate discrete rigid element models, such as Level Set Discrete Element Method (LSDEM) and “*Logiciel de Mécanique Gérant le Contact*” (LMGC90) [20], but not necessarily limited to them. The results of the most relevant experimental tests are commented and the importance of such a test campaign is discussed to investigate the real seismic behaviour of multi-blocks structures.

2. Previous studies

Doherty and Griffith [21–23] studied the seismic stability of multiple stacked concrete blocks structures considering the behaviour of an equivalent single block rigid body, subject to rocking and sliding phenomena. They used a tri-linear model to analyse the out-of-plane behaviour of this kind of structures, using a linearized method to describe the non-linear behaviour of discrete elements masonry structures.

Psycharis, Papastamatiou and Alexandris [14] analysed the seismic behaviour of a multi-block stone column of an ancient Greek temple through the study of a multi-drum column model and the simpler equivalent single-block model. They concluded that the single-block analysis was a first acceptable approximation to evaluate the seismic response of the structure but, to have complete and precise study, further and more complex analyses had to be done. Pitilakis, Tsinidis and Karafagka [24] analysed numerically and through real seismic tests on a shaking table the seismic behaviour of a multi-drum column. Their conclusions were validated by the experiments done on a real column. The need and the importance to validate complex numerical mechanical models to predict the seismic behaviour of multi-block structures through the use of shaking table tests has also been highlighted by Al Shawa, De Felice and others [25].

Harmon, Gabuchian and others [26] adopted the same approach to evaluate the seismic assessment of multi-block tower structures conceived to store energy. They developed both analytical and physical models to benchmark their assessment.

The purpose of mentioned tests at EUCENTRE is to physically analyse the seismic response of shielding blocks used as radiation protection for physical experiments, a domain little investigated in literature.

3. Shaking table tests

To calibrate the parameters of numerical models, a validation against the results of experimental tests is required. In particular, the seismic response and the stability of different configurations of stacked concrete blocks were studied through specifically designed dynamic tests on shaking table. The blocks used for these tests are made of reinforced concrete with dimensions $2.40 \times 1.60 \times 0.80$ m and weight 77 kN (Fig. 2), and are endowed with anchoring steel elements for their handling and transportation. The ones of these dimensions are the most used for radiation protection installations at CERN and they can be considered as a “standard”. Although some multiples and sub-multiples of this standard exist and are used at CERN, they were chosen as the most representative to be tested under seismic loads in EUCENTRE. The block configuration specimens were thought to investigate mainly the rocking behaviour of simple piles (Configurations 1 and 2) and, afterwards, the effect of a roof on top of them (Configuration 3 and 4). The blocks have been designed according to the EN 206–1 norms [27] and Eurocode 2 (EN 1992-1-1) [28]. Referring to the nomenclature adopted by such Norms, the main characteristics are: concrete quality C40/50, exposure class XC4-XD3-XF3, maximum diameter of the aggregates 32 mm, chloride content 0.20, metallic form-work type IV, edge chamfers 2 cm and reinforcement steel type B500B, characterized by a yielding stress greater than 500 MPa.

3.1. Test setup

Specimens of the four different configurations, whose height varied from 4.8 m to 7.4 m were built (Fig. 3). The first and the second specimen consisted of three and four stacked solid blocks, respectively.

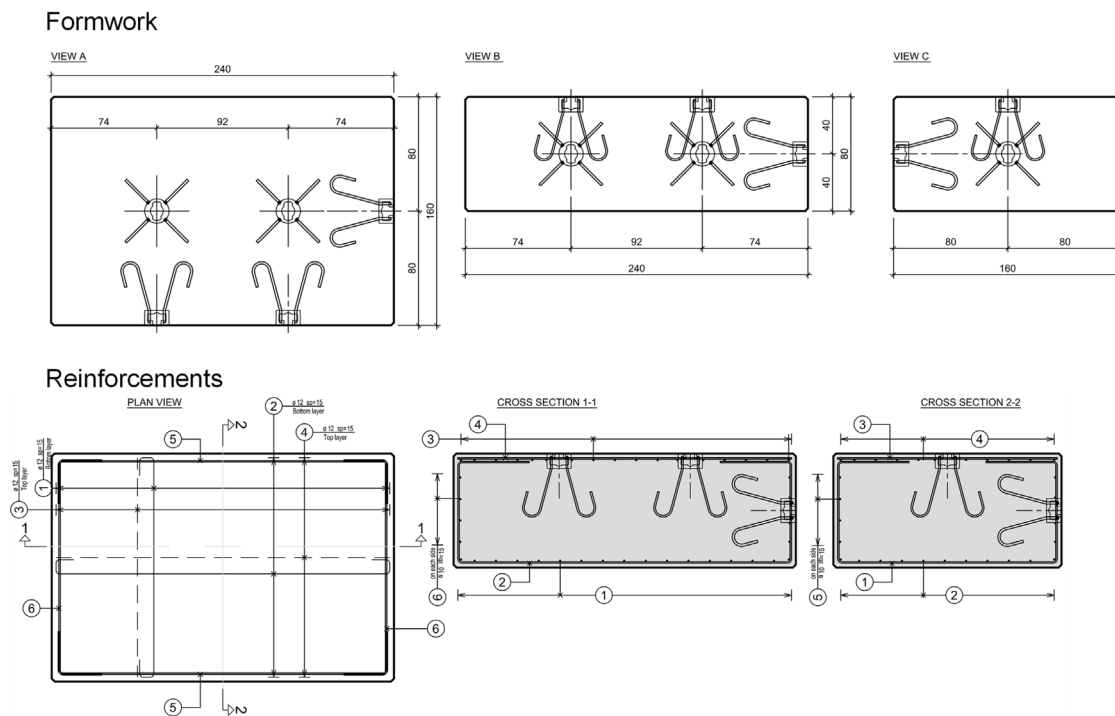


Fig. 2. Dimensions of CERN standard concrete blocks.

The third and the fourth ones consisted of two parallel walls of four stacked solid blocks, with an additional block placed at the top; in particular, in the fourth specimen, a system of four parallel steel profiles supported the top block. The steel profiles, which can be seen in Fig. 3, had I shaped sections with height 96 mm (European HEA geometrical type).

The specimens were assembled on the platform of an unidirectional shaking table. They were simply supported by a base concrete slab, whose translations were restrained by two steel profiles fixed to the platform of the shaking table. Undesired effects due to unexpected large displacements or rotations were prevented through retaining steel systems provided along the height of the specimens, designed to not affect the specimens during the tests (Fig. 4).

A detail of the retaining system along the height of the specimen is depicted in Fig. 5. It consists of two protruding bars partially embedded in the upper block and a system of steel profiles having a sort of “T” shape, fixed to the lower block. If excessive rotations occur, a bar is stopped by the steel system to avoid damages to the laboratory, as shown in Fig. 5. Actually, no interactions occurred between the retaining systems and the blocks during the experimental campaign.

The seismic input of the dynamic tests consisted of two different recorded acceleration time-histories, called Alkion and Basso Tirreno [29], applied at increasing amplitude levels at the base of the specimens. This input is an upper bound of the standard acceleration time-history representing the Geneva Area, according to the Swiss applicable norms [30]. The acceleration time-histories and their characteristics can be found in Fig. 6 and Table 1. More in detail, according to the test protocol, the initial intensity level was equal to 50% of the maximum acceleration (Peak Ground Acceleration (PGA)) characterizing each accelerogram. The successive tests had an amplitude increment of about 25% up to the achievement of an incipient instability condition of the specimens. At each new intensity level, the relative position of the blocks was checked and, in case of large misalignments, the specimen was restored to its initial configuration. Additional low intensity tests with sinusoidal waves characterized by constant amplitude and variable frequency (random wave tests) in the range 0–60 Hz, have been performed to assess the current dynamic properties of the specimens.

Table 1

Characteristics of the ground motions.

Earthquake	Date	Magnitude [Mw]	Distance [km]	PGA [m/s^2]
Alkion	02/25/1981	6.3	25	1.176
Basso Tirreno	04/15/1978	6	18	1.585

3.2. Measurements

The assessment of the dynamic properties and of the seismic response of the specimens were based on the spatial components of accelerations and displacements measured at different levels along the height of the specimens themselves. The specimens were equipped with up to 21 2g- and 6g-acceleration transducers, 4 displacement transducers and 101 retro-reflective optical markers, belonging to two different acquisition systems. Further data regarding force, accelerations, velocities and displacements of the shaking table came from both control system and additional transducers. The recording frequencies were 512 Hz and 200 Hz for accelerations and displacements, respectively. Moreover, the accelerations were filtered with a 50 Hz-low-pass filter, since the frequency response of the transducers was 0–200 Hz. Redundant measured displacements coming from both external acquisition systems and control system allowed data synchronization. Furthermore, 33 spatial displacement components were monitored for each block through retro-reflective markers; the common layout consisted of 5 + 5 markers distributed at the top and at the bottom levels along two orthogonal sides of the block, and one additional marker placed at the middle level of one side. The displacement transducers were used to check the relative displacements between the concrete basement and the shaking table. An example of the layout of the transducers is depicted in Figs. 7 and 8 for the specimen of Configuration 4.

3.3. Test results

As mentioned, each specimen was preliminarily subjected to investigations with “random tests” to determine their natural frequency of

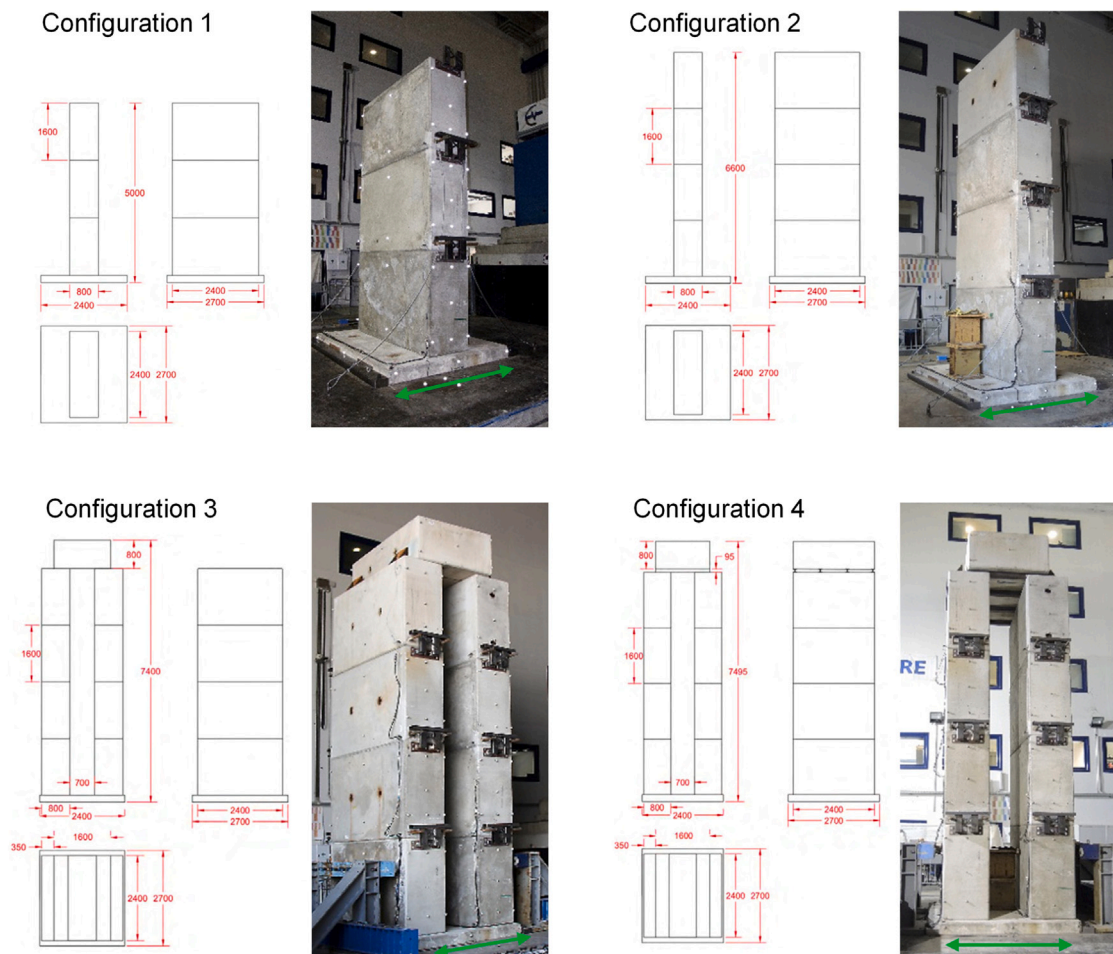


Fig. 3. Specimens of the four block configurations: (1) 4.8 m-height three-block specimen (2) 6.4 m-height four-block specimen; (3) 7.2 m-height nine-block 2-wall specimen; (4) 7.4 m-height nine-block 2-wall specimen with the top block supported by steel profiles. Lengths are in mm; the green double arrow indicates the direction of the base shaking.

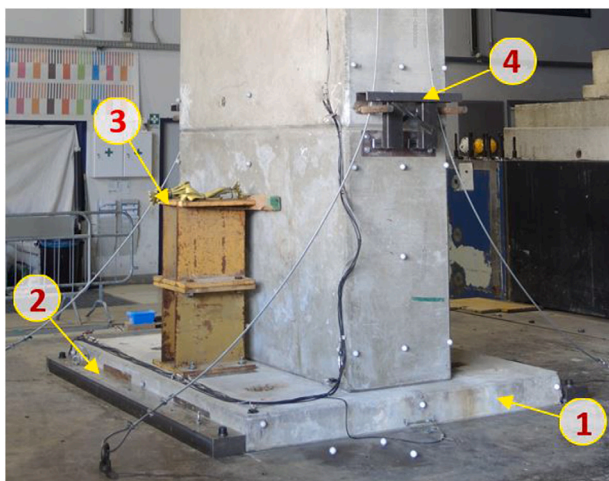


Fig. 4. Common details of each specimen: (1) concrete foundation slab, (2) steel profiles to inhibit the translation of the slab, (3) steel stoppers at the base, (4) steel retaining system between concrete blocks along the height of the specimen.

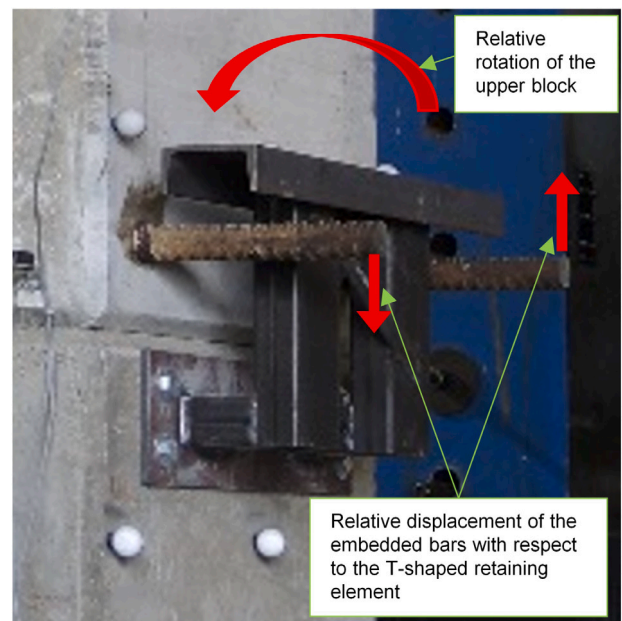


Fig. 5. Detail of the retaining systems along the height of the specimens, used only for safety reasons.

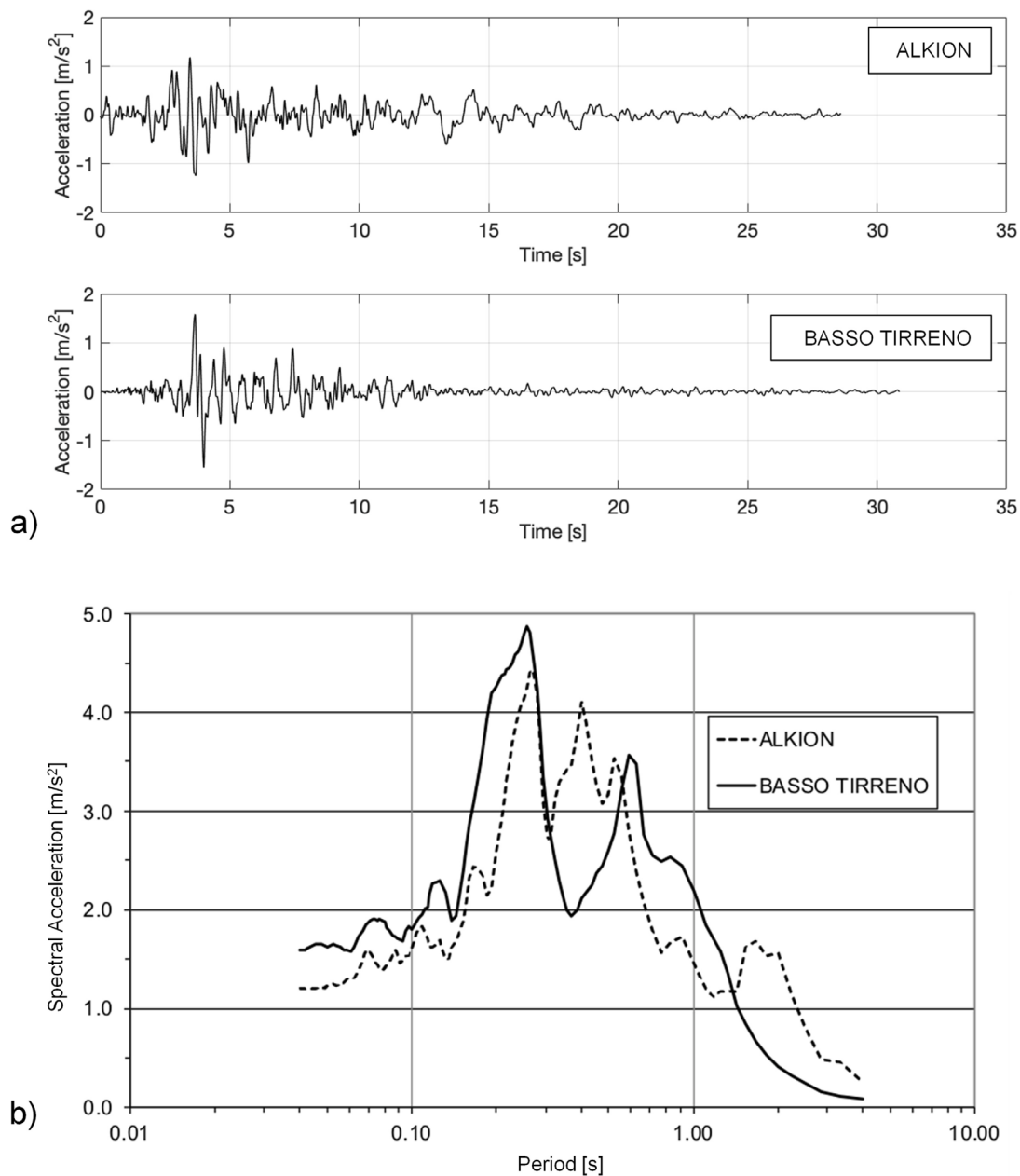


Fig. 6. Alkion and Basso Tirreno earthquakes: (a) horizontal acceleration time-histories and (b) spectral acceleration.

Table 2

Elastic frequency F_0 and period T_0 of the specimens.

Configuration	F_0 [Hz]	T_0 [s]
1	27.460	0.036
2	15.420	0.065
3	12.120	0.083
4	11.940	0.084

vibration. Such tests consisted of the imposition of an acceleration at the base at low constant intensity and variable frequency. The results are summarized in Table 2.

Regarding the main results of the tests, the specimen of Configuration 1 was subjected to 10 tests at different acceleration intensity levels, ranging from 0.035 g to 0.210 g (Alkion accelerogram) and from 0.037 g to 0.201 g (Basso-Tirreno accelerogram), as resumed in Table 3.

The displacement profiles were almost linear; at the maximum intensities, the specimen experienced maximum positive and negative top longitudinal displacements (relative to the base) of about 50 mm and -58 mm, respectively (Fig. 9). Since the blocks were simply supported, an incipient rocking mechanism was noticed during the tests at higher intensities, characterized by a maximum vertical detachment at the base of about 2–3 mm. No evident torsional mechanisms were noticed directly during the tests. The maximum horizontal acceleration amplifications on the specimen were 5.2 and 4.5 for Alkion and Basso-Tirreno accelerograms, respectively; the corresponding vertical amplifications were 80% and 120% of the horizontal ones.

Specimen of Configuration 2 was subjected to 10 tests ranging from 0.037 g to 0.136 g (Alkion accelerogram) and from 0.032 g to 0.101 g (Basso Tirreno accelerogram), as summarized in Table 4. The displacement profiles were almost linear, but not symmetric when the Alkion accelerogram was applied; the maximum negative relative

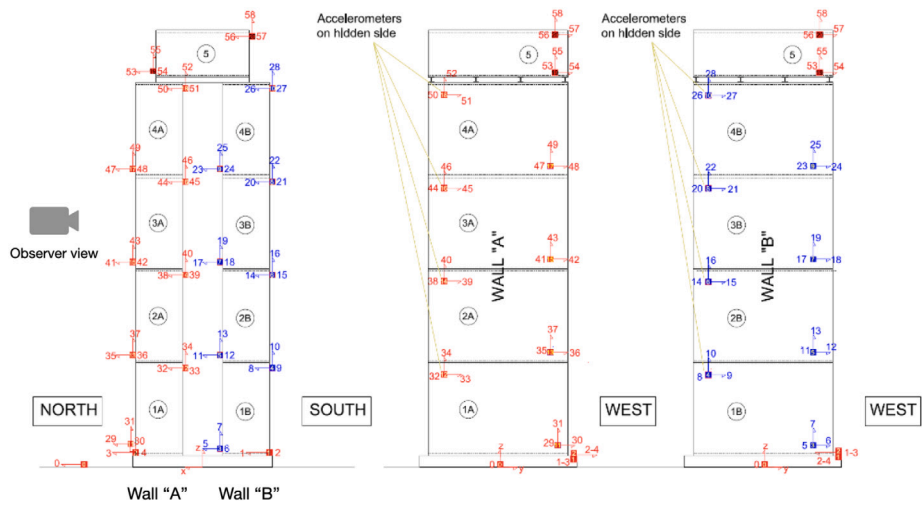


Fig. 7. Specimen of Configuration 4: layout of the accelerometers (left) with Wall A (middle) and Wall B (right) from the observer view respectively.

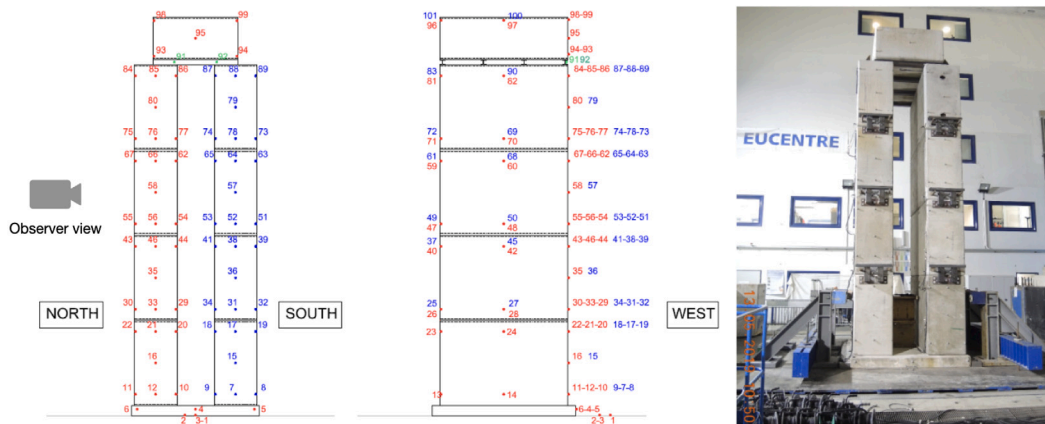


Fig. 8. Specimen of Configuration 4: layout of the retro reflective markers (left) with side view of the structure (middle) from the observer view.

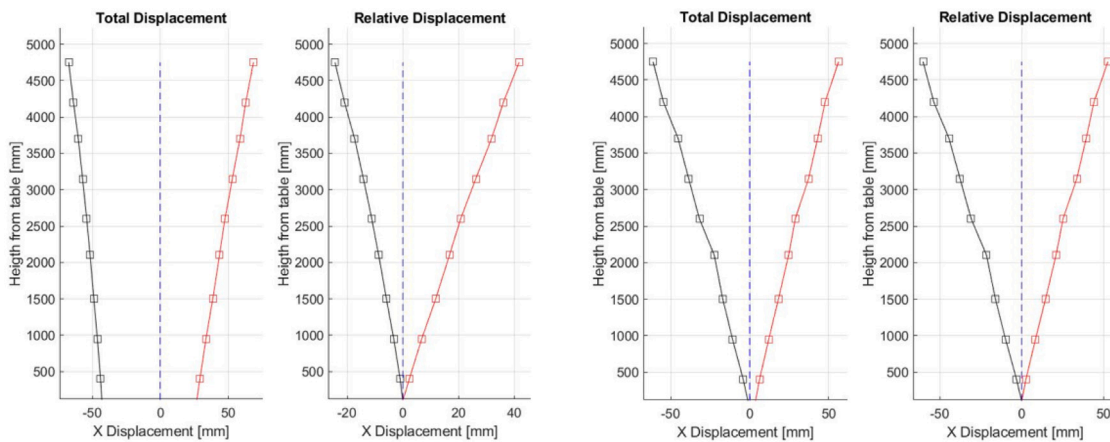


Fig. 9. Configuration 1: specimen total and relative displacement profiles corresponding to the attainment of the maximum acceleration intensities (0.21 g, Alkion accelerogram (left) and 0.20 g, Basso-Tirreno accelerogram (right)). Displacement profiles were obtained at three different levels of a block (see Fig. 8 as an example), hence nine data points in total per single wall.

displacement at the top was greater than the positive one (ratio of about 1.5) at 0.105 g, whilst the positive displacement was twice the negative one at 0.126 g. At the maximum intensities, the specimen experienced maximum positive and negative top longitudinal displacements (relative to the base) of 44 mm and -23 mm, respectively (Fig. 10) and an incipient rocking mechanism at the base was noticed, with a vertical

detachment at the base less than 2 mm. The maximum horizontal acceleration amplifications on the specimen were 4.9 and 7.5 for Alkion and Basso-Tirreno accelerograms, respectively; the corresponding vertical amplifications were 1.3 and 0.9 times the horizontal ones.

Specimen of Configuration 3 was subjected to 13 tests at different acceleration intensity levels ranged from 0.105 g to 0.210 g and from

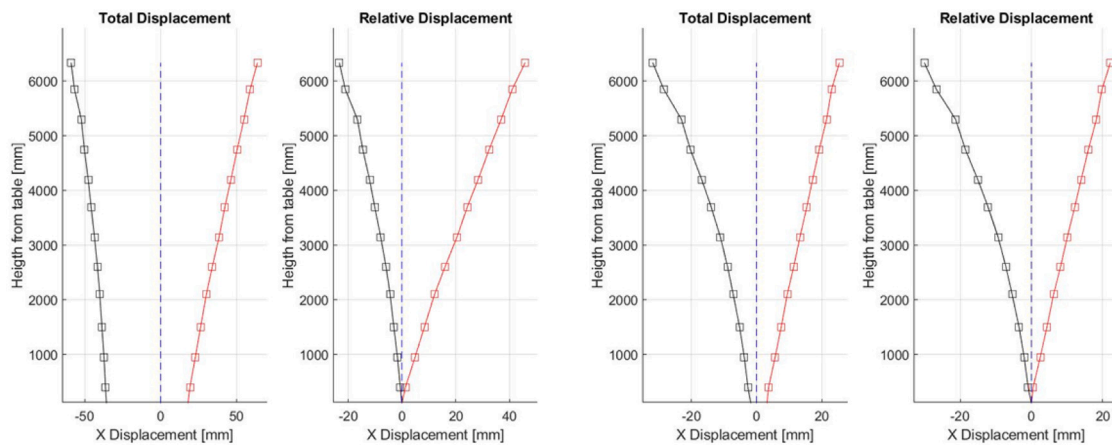


Fig. 10. Configuration 2: specimen total and relative displacement profiles corresponding to the attainment of the maximum acceleration intensities (0.136 g, Alkion accelerogram (left) and 0.101 g, Basso-Tirreno accelerogram (right)).

Table 3
Sequence of tests carried out on the specimen of Configuration 1.

N.	ID	Input type	Acceleration at the base of the specimen [g]
1	-	Random wave test	-
2	1AL1	ALKION	0.035
3	1AL2	ALKION	0.086
4	1AL3	ALKION	0.105
5	-	Random wave test	-
6	1AL4	ALKION	0.157
7	1AL5	ALKION	0.210
8	1BT6	BASSO-TIRRENO	0.037
9	1BT7	BASSO-TIRRENO	0.070
10	1BT8	BASSO-TIRRENO	0.101
11	1BT9	BASSO-TIRRENO	0.151
12	1BT10	BASSO-TIRRENO	0.201

Table 4
Sequence of tests carried out on the specimen of Configuration 2.

N.	ID	Input type	Acceleration at the base of the specimen [g]
1	-	Random wave test	-
2	1AL1	ALKION	0.037
3	1AL2	ALKION	0.071
4	1AL3	ALKION	0.105
5	1AL4	ALKION	0.115
6	1AL5	ALKION	0.126
7	1BT6	ALKION	0.1367
8	1BT7	BASSO-TIRRENO	0.032
9	1BT8	BASSO-TIRRENO	0.056
10	1BT9	BASSO-TIRRENO	0.091
11	1BT10	BASSO-TIRRENO	0.101

0.101 g to 0.181 g for Alkion and Basso Tirreno accelerograms, respectively (see Table 5 for more details). Its response was characterized by the following peculiarities: (i) the maximum horizontal acceleration amplifications on the specimen were 1.7 g and 1.8 g for Basso-Tirreno and Alkion accelerograms, respectively; the vertical components were 75% of the horizontal ones; (ii) the displacement profiles of the two walls were quite similar, in particular they were quite linear and symmetric for intensities lower than 90% of the PGA of the Alkion accelerogram; after that, unsymmetrical positive and negative maximum displacement profiles were observed; (iii) the maximum positive and negative relative displacements at the top of the walls (excluding the block at the top) were approximately 62 mm and -53 mm for the left wall and 62 mm and -55 mm for the right wall (Fig. 11); (iv) the block at the top performed relevant relative torsional rotations with respect to the two walls at high PGA intensities (Fig. 12); (v) A rocking

Table 5
Sequence of tests carried out on the specimen of Configuration 3.

N.	ID	Input type	Acceleration at the base of the specimen [g]
1	-	Random wave test	-
2	1AL1	ALKION	0.105
3	1AL2	ALKION	0.146
4	1AL3	ALKION	0.147
5	1AL4	ALKION	0.157
6	1AL5	ALKION	0.168
7	1BT6	ALKION	0.189
8	1BT7	ALKION	0.210
9	1BT8	BASSO-TIRRENO	0.101
10	1BT9	BASSO-TIRRENO	0.121
11	1BT10	BASSO-TIRRENO	0.141
12	1BT10	BASSO-TIRRENO	0.151
13	1BT10	BASSO-TIRRENO	0.161
14	1BT10	BASSO-TIRRENO	0.181

mechanism at the base was noticed during the tests, especially at higher intensities; the maximum vertical detachment at the base was of 2 mm; (vi) a slight torsional mechanism was developed during the tests (the relative rotation of the block at the top was about 5 degrees after the last test with Alkion accelerogram).

Finally, specimen of Configuration 4 was subjected to 12 tests at different acceleration intensity levels ranged from 0.105 g to 0.210 g and from 0.101 g to 0.151 g for Alkion and Basso-Tirreno accelerograms, respectively (see Table 6 for more details). The response of the specimen may be summarized as follows: (i) the displacement profiles of the two walls differed and became not symmetrical at higher intensity levels; (ii) the displacement profiles were heavily conditioned by relevant resonance effects arisen when Alkion accelerogram was applied; when the resonance effects did not arise (Basso-Tirreno accelerogram), maximum top displacements of approximately ± 50 mm (excluding the top block) were noticed for both walls, otherwise the displacements were unsymmetrical and increased up to +380 mm and -310 mm for both walls (Fig. 13); (iii) without resonant effects, the maximum horizontal acceleration amplification on the specimen was about 2, otherwise it achieved values greater than 5; (iv) also in case of resonance effects, the maximum vertical acceleration were still comparable to the horizontal one (about 1.10 g for both components); (v) the top block performed significant relative displacements and rotations at high PGA intensities and a slight torsional mechanism was developed during the tests; (vi) a rocking mechanism at the base developed, especially at higher intensities, with maximum vertical detachment at the base greater than 10 mm.

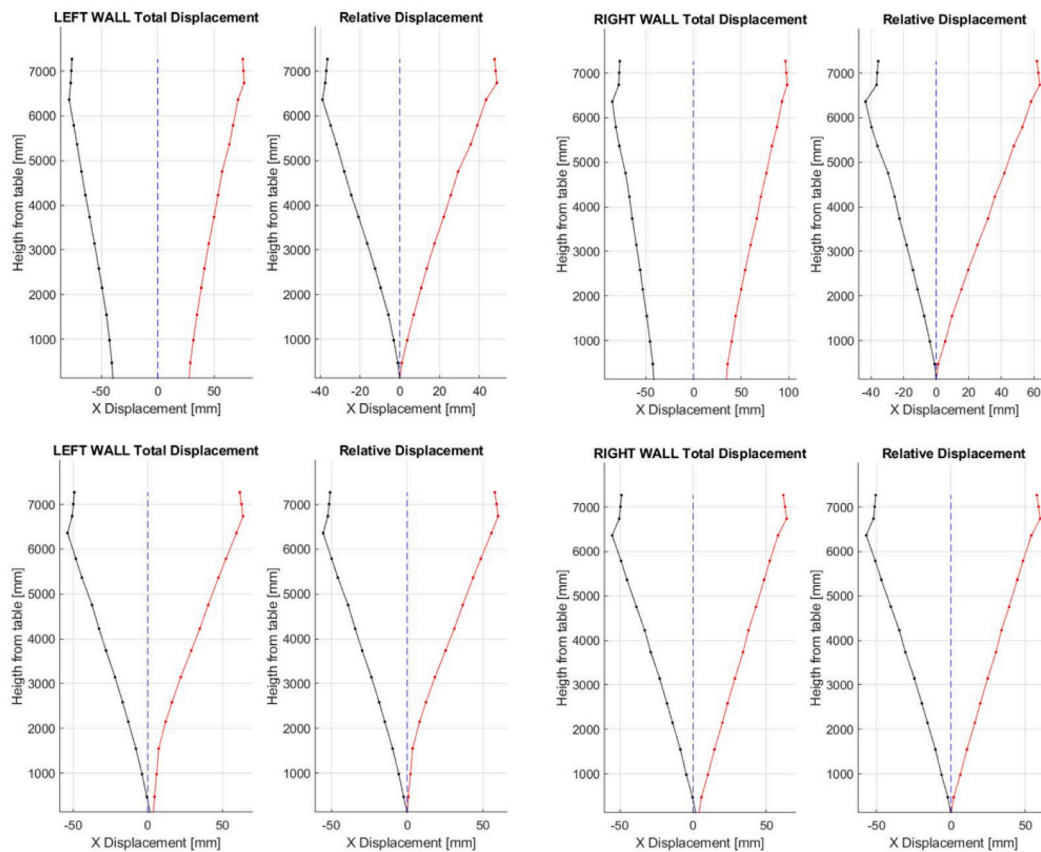


Fig. 11. Configuration 3: specimen total and relative displacement profiles corresponding to the attainment of the maximum acceleration intensities (top: 0.210 g, Alkion accelerogram; bottom: 0.181 g, Basso-Tirreno accelerogram).

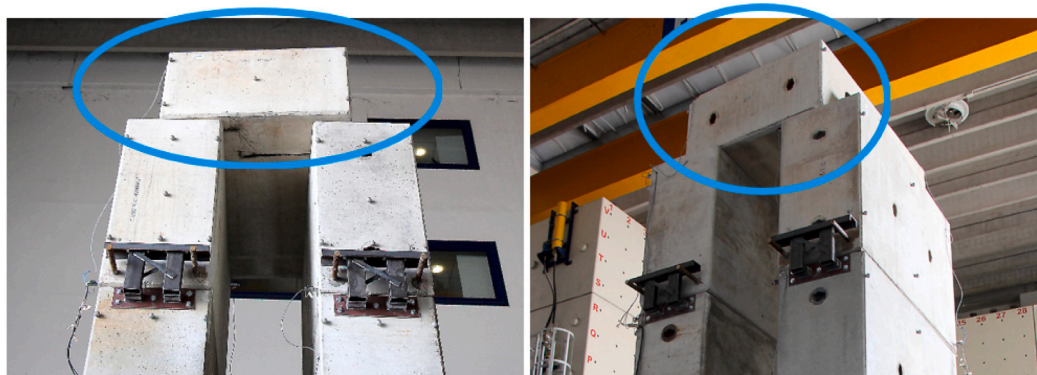


Fig. 12. Configuration 3: relative rotation of the block at the top of the specimen at the end of the tests with Alkion accelerogram.

4. Discussion

The comparisons in terms of maximum and minimum top displacements (Fig. 14), top accelerations (Fig. 16) and shear action at the base (Fig. 17) as a function of the acceleration applied at the base are briefly discussed in this section. The relation between peak displacements and acceleration at the base (Fig. 14) tended to be not linear already at medium acceleration intensities, but substantially only for the first the specimens of the Configurations 1 and 2. The specimens of Configurations 3 and 4 had similar responses, except for the resonant effects regarding the latter at the highest intensity. The reason why the resonance effects occurred on Configuration 4 lies in the dynamic characteristics of its specimen combined with the intensity of the acceleration at the base and the characteristics of the Alkion accelerogram. The initial period of the specimen was 0.084

s. During the dynamic tests, the specimen started oscillating and a rocking mechanism occurred, which increased the period to values where the spectral amplification at the base is relevant; the spectrum of Alkion has acceleration peaks of 0.71 g at 0.27 s and 0.68 g at 0.40 s (Fig. 15). When the period of the specimen reached the values corresponding to these peaks, the resonance effects started, generating relevant oscillations for several seconds even when the shaking table stopped. For what concerns the Basso-Tirreno accelerogram, it was applied up to an acceleration at the base of 0.151 g. This implies that the spectra at the base had a minor peak of 0.4 g at 0.28 s and no peaks between 0.35 s and 0.55 s (Fig. 15). These conditions did not generate resonance effects on the same specimen. The reason why no resonance effects occurred in all the other cases, especially for Alkion accelerogram, is probably related to the fact that the period of

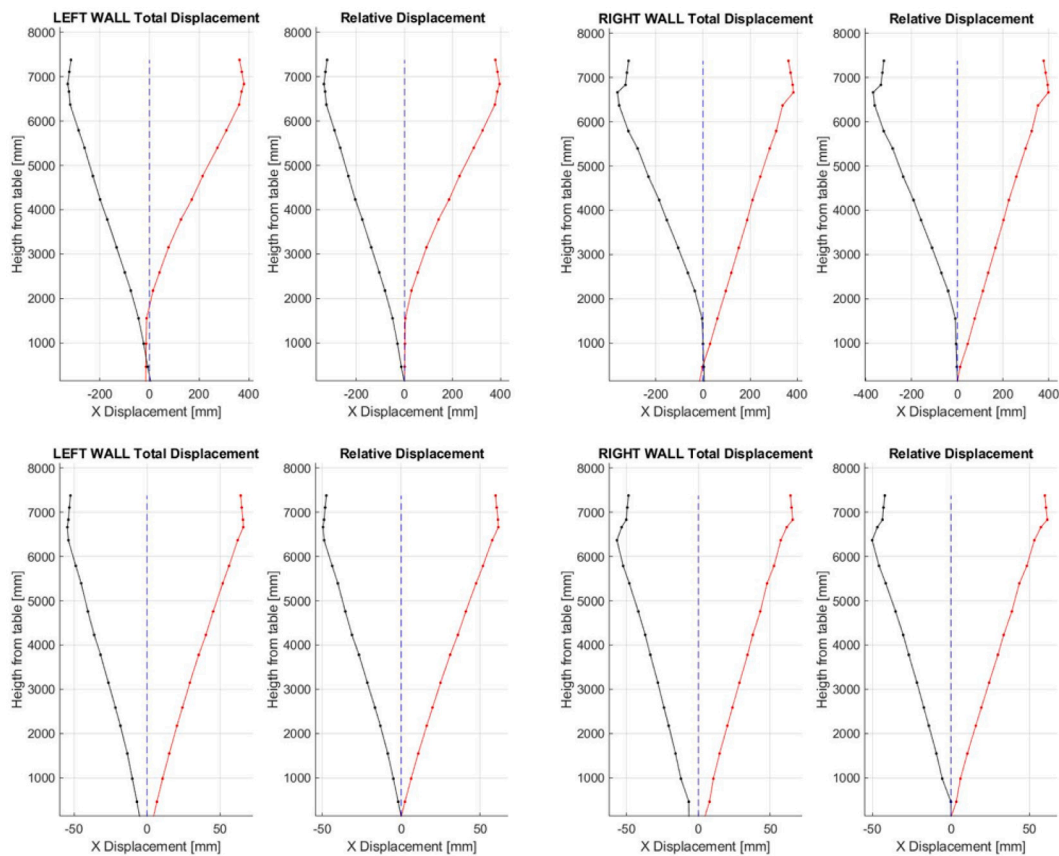


Fig. 13. Configuration 4: specimen displacement profiles. Last iterations of Alkion 100% (top) and Basso Tirreno 100% (bottom).

Table 6
Sequence of tests carried out on the specimen of Configuration 4.

N.	ID	Input type	Acceleration at the base of the specimen [g]
1	-	Random wave test	-
2	1AL1	ALKION	0.105
3	1AL2	ALKION	0.146
4	1AL3	ALKION	0.147
5	1AL4	ALKION	0.157
6	1AL5	ALKION	0.168
7	1BT6	ALKION	0.189
8	1BT7	ALKION	0.210
9	1BT8	BASSO-TIRRENO	0.101
10	1BT9	BASSO-TIRRENO	0.121
11	1BT10	BASSO-TIRRENO	0.141
12	1BT10	BASSO-TIRRENO	0.151
13	1BT10	BASSO-TIRRENO	0.161
14	1BT10	BASSO-TIRRENO	0.181

the specimens increased without reaching the values associated to the major peaks of the spectrum.

The acceleration at the top of the specimens, compared to the acceleration at the base (Fig. 16), increased not linearly for medium-high intensities. In particular the specimen of Configuration 1 was subjected to amplifications up to 5.2 and 4.5 for Alkion and Basso-Tirreno accelerograms, respectively. The maximum amplifications on the specimen of Configuration 2 were of 4.9 and 7.5. The results of the tests on the specimen of Configuration 3 gave a measure of the possible amplifications on the double pile configurations (with nine blocks) without resonance effects; with Alkion accelerogram, the maximum amplification was 11.7 at low intensities, then its values were between 6.0 and 10.0. In the case of the tests with Basso-Tirreno accelerogram, the amplification was between 8.9 and 11.6, with the maximum value

at the highest intensity. The resonance effects (specimen of Configuration 4, Alkion accelerogram) imposed an amplification up to 35.0. No resonance effects occurred on the specimen of Configuration 4 with Basso-Tirreno Accelerogram, the maximum amplification was equal to 13.0.

The shear action at the base (Fig. 17) was calculated as a function of the distribution of the acceleration along the height of the specimens and the mass of the blocks. Maximum values of 60 kN were determined for the specimens of Configurations 1 and 2. Some uncertainties are associated to the calculation method in the case of the double pile configurations with nine blocks, due to the configurations themselves and to the rocking mechanism which was triggered.

5. Findings and conclusions

This paper describes the shaking table tests carried out at EUCENTRE to investigate the seismic behaviour of four different configurations of full scale stacked concrete blocks, not connected, simply supported by each other. The acceleration time-histories of two different earthquakes have been used. The specimens of each configuration have been tested several times at increasing amplitudes until some rocking or sliding mechanisms have been triggered. The paper treats a type of structure in a domain – seismic response of shielding installations for radiation protection in nuclear research institutions – little investigated in literature.

The main conclusions of the testing campaign can be summarized in the following points:

- the two main phenomena that can be noticed with this type of comprised of sliding and rocking. A rocking mechanism at the base was noticed during the tests, especially at higher intensities of seismic action;

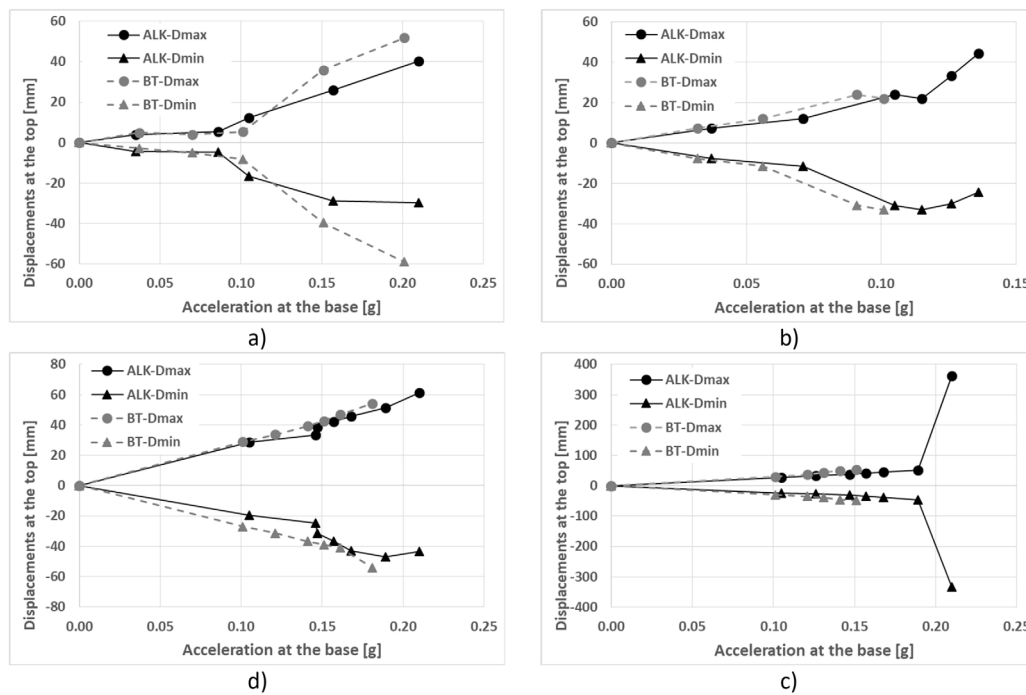


Fig. 14. Maximum and minimum displacements at the top of the specimens as a function of the level of acceleration at the base at each test and of the applied acceleration (ALK = Alkion, BT = Basso-Tirreno). (a) Configuration 1; (b) Configuration 2; (c) Configuration 3, the displacement is the average value at the top of the two walls; (d) Configuration 4, the displacement is the average value at the top of the two walls.

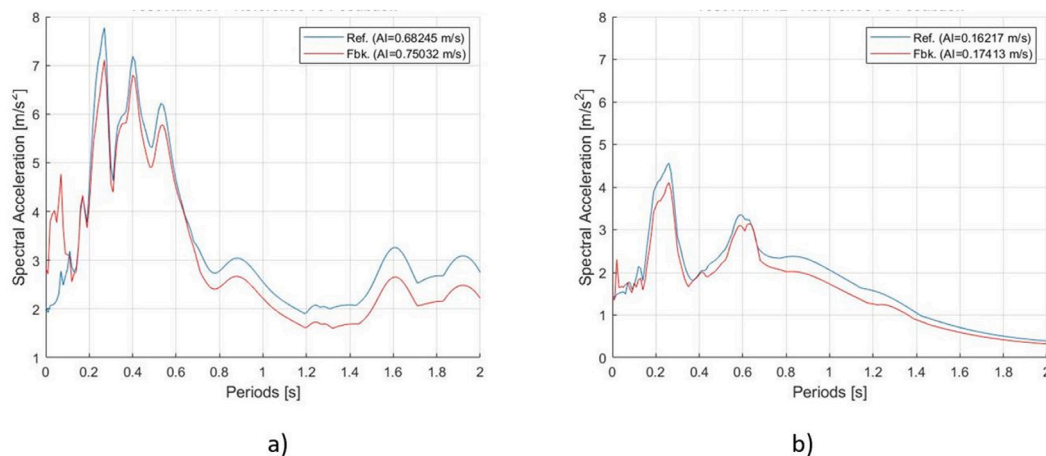


Fig. 15. Configuration 4: comparison between reference command and feedback signal in terms of acceleration spectrum at the base of the specimen for (a) Alkion (acceleration level of 0.210 g, last test) and (b) Basso-Tirreno (0.151 g, last test) accelerograms.

- other rocking mechanisms were noticed between the blocks for the highest configurations and the highest seismic actions;
- the lateral displacement at the top of each configuration was proportional to the height of the configuration itself and the intensity of the seismic action;
- for Configuration 4, the block at the top of the specimen performed relevant relative displacements and rotations with respect to the two walls at high PGA intensities. The fact of having introduced the four steel beams between the roof block and the columns, which is the sole difference between Configurations 3 and 4, increased the relative maximum displacement with a ratio of approximately 3.50 with respect to Configuration 3 (10 cm);
- these data constitute an important source to calibrate different discrete element models to study the seismic response of shielding multi-block installations used for radiation protection in particle physics research institutions like CERN.

Declaration of competing interest

The authors declare that they have no known competing financial interests or personal relationships that could have appeared to influence the work reported in this paper.

Data availability

Data will be made available on request.

Acknowledgement

The Authors would like to acknowledge CERN - Site and Civil Engineering Department (SCE), which funded the experimental tests presented in this paper.

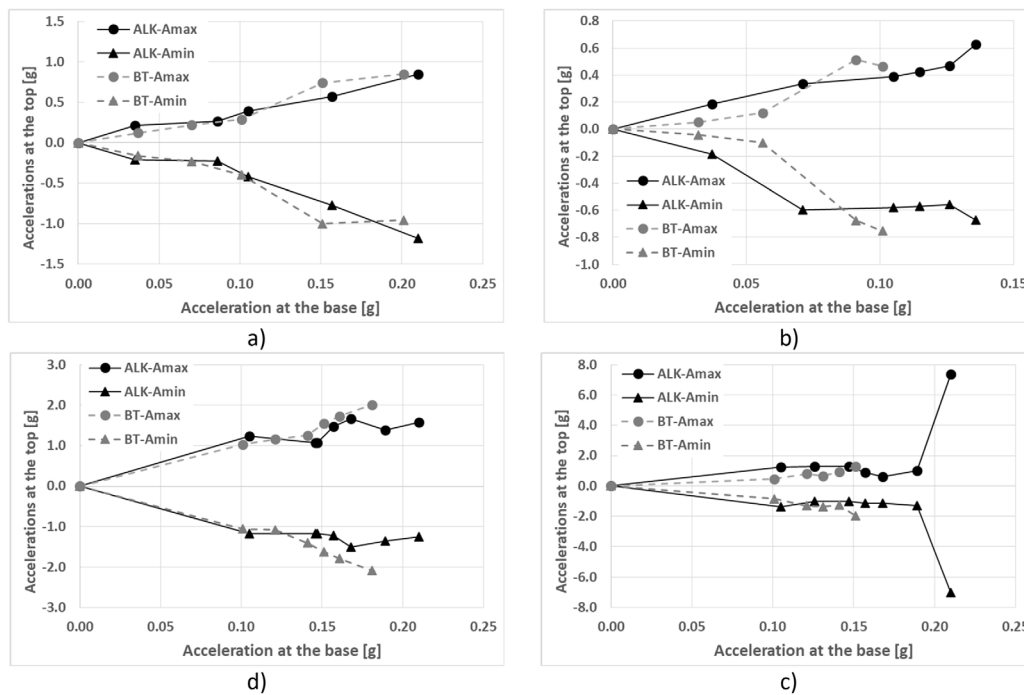


Fig. 16. Maximum and minimum accelerations at the top of the specimens as a function of the level of acceleration at the base at each test and of the applied acceleration (ALK = Alkion, BT = Basso-Tirreno). (a) Configuration 1; (b) Configuration 2; (c) Configuration 3; (d) Configuration 4.

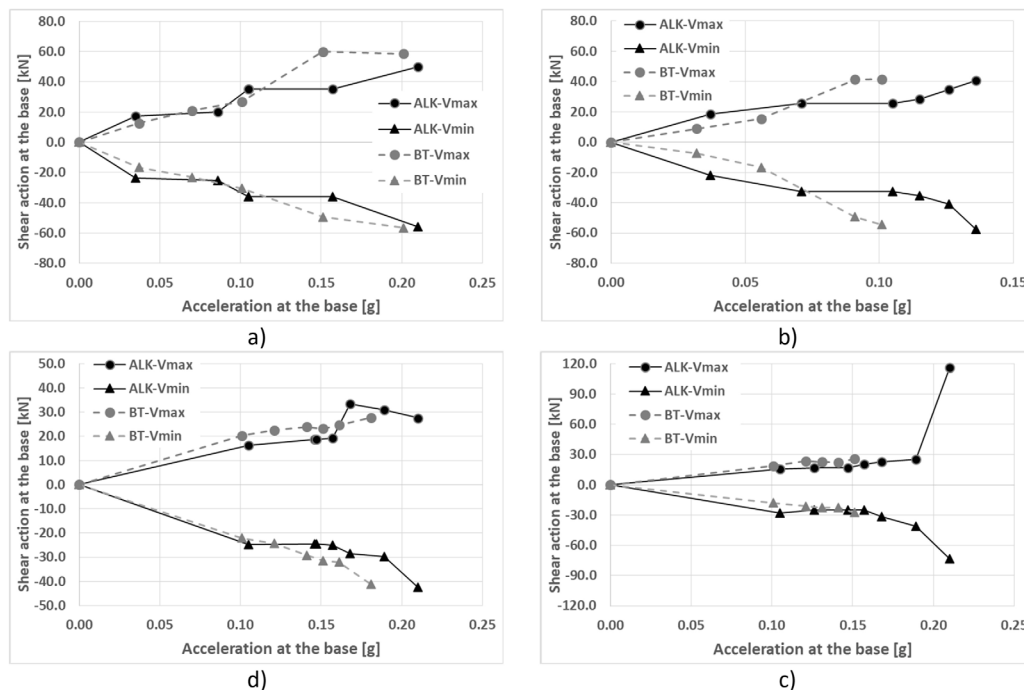


Fig. 17. Maximum and minimum shear action at the base of the specimens as a function of the level of acceleration at the base at each test and of the applied acceleration (ALK = Alkion, BT = Basso-Tirreno). (a) Configuration 1; (b) Configuration 2; (c) Configuration 3; (d) Configuration 4.

References

[1] EN 1998-1:2004 - eurocode 8 - design of structures for earthquake resistance - Part 1 : General rules, seismic actions and rules for buildings. European Committee for Standardization (CEN).

[2] Grünthal G, Musson RMW, Schwarz J, M. Stucchi. European macroseismic scale 1998, EMS-98. In: Cahiers du centre européen de géodynamique et de séismologie, volume 19. Luxembourg 2001: Conseil de l'Europe; 2001.

[3] Aslam M, Godden WG, Scalise DT. Earthquake rocking response of rigid bodies. J Struct Eng ASCE 1980;v.106(2):377-92.

[4] Augusti G, Sinopoli A. Modelling the dynamics of large block structures. In: Calladine CR, editor. Masonry construction. Dordrecht: Springer; 1992.

[5] Ishiyama Y. Motions of rigid bodies and criteria for overturning by earthquake excitations. Earthq Eng Struct Dyn 1982;v.10:635-50.

[6] Lipscombe PR, Pellegrino S. Free rocking of prismatic blocks. J Eng Mech 1993;v.119(7):1387-410. [http://dx.doi.org/10.1061/\(ASCE\)0733-9399\(1993\)119:7\(1387\)](http://dx.doi.org/10.1061/(ASCE)0733-9399(1993)119:7(1387)).

[7] Olsen BE, Neylan AJ, Gorcholt W. Seismic test on a one-fifth scale HTGR core model. Nucl Eng Des 1976;v.36:355-65.

- [8] Sinopoli A. Dynamics and impact in a system with unilateral constraints the relevance of dry friction. *Meccanica* 1987;V.22:210–5.
- [9] Sinopoli A, Sepe V. Coupled motion in the dynamic analysis of a three block structure. *Appl Mech Rev* 1993;v.46(11S):S185–97. <http://dx.doi.org/10.1115/1.3122636>.
- [10] Spanos PD, Koh AS. Rocking of rigid blocks during harmonic shaking. *J Eng Mech* 1984;v.110(11):1627–42.
- [11] Stronge WJ. Rigid body collisions with friction. *Proc R Soc Lond Engl A* 1990;v.431:169–81.
- [12] Tso WK, Wong CM. Steady state rocking response of rigid blocks. part 1: analysis. *Earthq Eng Struct Dyn* 1989;v.18:89–120.
- [13] Dimitrakopoulos E, DeJong M. Revisiting the rocking block: the closed-form solutions and similarity laws. *Proc R Soc Lond Ser A Math Phys Eng Sci* 2012.
- [14] Psycharis IN, Papastamatiou DY, Alexandris AP. Parametric investigation of the stability of classical columns under harmonic and earthquake excitations. *Earthq Eng Struct Dyn* 2000;29:1093–109.
- [15] Makris N, Roussos Y. Rocking response and overturning of equipment under horizontal pulse-type motions. Peer center, Report (1998) / 5 OCT.1998, Berkeley: University of California; 1998.
- [16] Makris N, Zhang J. Rocking response and overturning of equipment. Peer center Report (2000) / 13, Berkeley: University of California.
- [17] Jean M, Moreau JJ. Unilaterality and dry friction in the dynamic of rigid body collections. In: Curnier A, editor. *Proc. contact mechanics int. symp.* 1992, p. 31–48.
- [18] Jean M. The non-smooth contact dynamic method. *Comput Methods Appl Mech Engrg* 1999;177(3–4):235–57.
- [19] Dubois F, Jean M. LMGC90 : une plateforme de développement dédiée à la modélisation des problèmes d'interaction. In: *Proc. 6ème colloque national en calcul des structures, giens, volume 1.* 2003, p. 111–8.
- [20] Zhou Z, Andreini M, Sironi L, Lestuzzi P, Andò E, Dubois F, Bolognini D, Dacarro F, Andrade J. Discrete structural systems modeling: Benchmarking of LS-DEM and LMGC90 with seismic experiments. *Journal of Engineering Mechanics* 2023. submitted for publication.
- [21] Doherty K, Griffith MC, Lam N, Wilson J. Displacement-based seismic analysis for out-of-plane bending of unreinforced masonry walls. *Earthq Eng Struct Dyn* 2002;31(4):833–50.
- [22] Doherty K, Rodolico B, Lam N, Wilson J, Griffith MC. The modelling of earthquake induced collapse of unreinforced masonry walls combining force and displacement principals. In: *12WCEE Proceedings, Paper 1645.*
- [23] Griffith MC, Lam N, Wilson J, Doherty K. Experimental investigation of unreinforced brick masonry walls in flexure. *ASCE J Struct Eng* 2004;130(3):423–32.
- [24] Ptilakis K, Tsinidis G, Karafagka S. Analysis of the seismic behavior of classical multi-drum and monolithic columns. *Bull Earthq Eng* 2017;15:5281–307.
- [25] Al Shawa O, De Felice G, Mauro A, Sorrentino L. Out-of-plane seismic behaviour of rocking masonry walls. *Earthq Eng Struct Dyn* 2012;41(5):949–68.
- [26] Harmon John M, Gabuchian Vahe, Rosakis Ares J, Conte Joel P, Restrepo Jose I, Rodriguez Andres, Nema Arpit, Pedretti Andrea R, Andrade Jose E. Predicting the seismic behavior of multiblock tower structures using the level set discrete element method. 2022.
- [27] EN 206-1:2000 - Concrete - Part 1 : Specification, Performance, Production and Conformity. European Committee for Standardization (CEN).
- [28] EN 1992-1-1:2004 - Eurocode 2 - Design of Concrete Structures - Part 1-1 : General Rules and Rules for Buildings. European Committee for Standardization (CEN).
- [29] Ambraseys N, Smit P, Sigbjornsson R, Suhadolc P, Margaris B. Internet-site for european strong-motion data, european commission, research-directorate general. Environment and Climate Programme; 2002.
- [30] SIA 261/2020 : actions sur les structures porteuses. Swiss Society of Engineers and Architects, In French.